Increase in spin injection efficiency of a CoFe/MgO(100) tunnel spin injector with thermal annealing

R. Wang,[a] X. Jiang, R. M. Shelby, R. M. Macfarlane, and S. S. P. Parkin[b]
IBM Research Division, Almaden Research Center, San Jose, California 95120

S. R. Bank and J. S. Harris
Solid State and Photonics Laboratory, Stanford University, Stanford, California 94305

Postgrowth thermal annealing of a CoFe/MgO(100) tunnel spin injector grown on a GaAs/AlGaAs quantum well structure results in a significantly increased spin injection efficiency as inferred from the polarization of heavy-hole electroluminescence from a quantum well optical detector. The as-deposited sample displayed an initial polarization at 100 K of 43%, which was increased to 52% after a 1 h anneal at 300 °C, and finally to 55% after a second 1 h anneal at 340 °C. The polarization remained unchanged upon further annealing to temperatures as high as 400 °C. These results show that tunnel spin injectors based on CoFe/MgO are robust with high thermal stability, making them useful for device applications. © *2005 American Institute of Physics*. [DOI: 10.1063/1.1787896]

The pursuit of electronic devices with enhanced functions deriving from the manipulation of electron spin has created a field of "spintronics." Manipulation of spin states within metals and semiconductors has the potential to produce sensors, memory, and circuit components that could provide nonvolatility, increased speed, and density, and decreased power consumption as compared to existing charge-based technologies.[1–3] In recent years there has been much focus on the creation of populations of spin-polarized carriers inside semiconductors, since this is the first step towards the development of semiconductor spintronic devices. Initial work using diluted magnetic semiconductors at low temperatures demonstrated highly efficient spin injection into semiconductors.[4–6] However, the low magnetic ordering temperatures of these materials make them less attractive than injectors using traditional ferromagnetic (FM) metals, which have Curie temperatures well above room temperature. While the conductivity mismatch between such metals and semiconductors may limit spin injection efficiency in the diffusive regime,[7] transport in the tunneling regime overcomes this obstacle.[8] Indeed, several groups have successfully injected electron currents with high spin polarizations into semiconductors using tunneling contacts between FM metals and semiconductors.[9–14]

A key characteristic of a spin injector is its tunneling spin polarization (TSP), which determines the maximum possible spin polarization of the current injected into the semiconductor. The TSP will depend significantly on the tunnel barrier material and structure.[15,16] In particular, theoretical modeling by Butler *et al.*[15] revealed that the tunneling conductance in an Fe/MgO(100) structure is dominated by the majority spin Δ_1 state, which decays slowly inside the crystalline MgO barrier along the (100) direction, thereby giving rise to highly spin-polarized tunneling current. Indeed, Fe/MgO/Fe tunnel junctions have been predicted to display tunneling magnetoresistance (TMR) values as high as 1000%.[16] Experimental studies motivated by these predictions have shown TMR values exceeding 220% at room temperature and tunneling spin-polarization values of up to 85% in tunnel junctions using MgO, far outperforming conventional junctions with Al_2O_3 barriers.[2] In this letter, we demonstrate that highly spin-polarized current injection from CoFe/MgO injectors into GaAs is significantly improved by thermal anneal treatments and that these tunnel spin injectors show remarkable thermal stability to temperatures up to 400 °C.

In these experiments, the semiconductor light-emitting diode for spin detection was grown by molecular beam epitaxy with the following structure: p^+-GaAs(100) substrate/570 nm p-$Al_{0.08}Ga_{0.92}As$ buffer layers with a stepped doping profile/75 nm i-$Al_{0.08}Ga_{0.92}As$/10 nm i-GaAs/15 nm i-$Al_{0.08}Ga_{0.92}As$/100 nm n-$Al_{0.08}Ga_{0.92}As$ ($n \sim 5 \times 10^{16}$ cm^{-3})/5 nm i-GaAs. The sample was then capped with an arsenic protective layer and transported in air to a magnetron-sputtering chamber where the tunnel spin injector was grown. Prior to growth, the sample was heated to 550 °C to remove the arsenic cap, and then cooled to room temperature for deposition. Shadow masks were used to deposit ~3 nm MgO barriers followed by 5 nm CoFe ferromagnetic emitter electrodes. Finally, a 10 nm Ta layer was grown to protect the emitter from oxidation. The final spin injector structure had an active area of ~100×300 μm^2. The postgrowth anneals were conducted in a high vacuum annealing furnace for 1 h at the selected anneal temperatures.

The electroluminescence (EL) measurements utilize a superconducting magnet cryostat with optical access, to allow for the measurement of the polarization of light emitted from the GaAs/AlGaAs quantum well. A magnetic field was applied perpendicular to the film plane. The EL signal was detected from the front side of the sample through the CoFe/MgO injector. In this Faraday geometry, the optical selection rules provide a direct correlation between the EL polarization and the spin polarization of the electrons just prior to recombination.[17] A bias voltage (V_T) applied between the back side of the semiconductor wafer and the

---

[a] Also at Solid State and Photonics Laboratory, Stanford University, Stanford, California 94305.
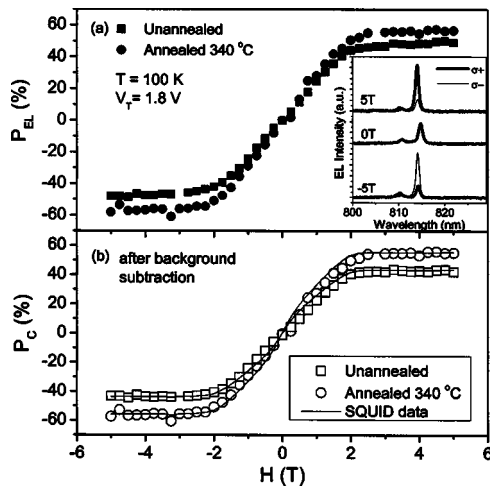[b] Author to whom correspondence should be addressed. Electronic mail: parkin@almaden.ibm.com

FIG. 1. Magnetic-field dependence of P_{EL} (a) and P_C (b) at 100 K with $V_T = 1.8$ V for the measured EL polarization before annealing (■) and after annealing at 340 °C (●). The current was 0.12 mA before anneal and 0.1 mA after the 340 °C anneal. Inset in (a) are typical EL spectra (here, taken after the 340 °C anneal) at −5, 0, 5T, where bold and thin black lines represent the left (σ+) and the right (σ−) circular polarization components, respectively. The solid lines in (b) represent the CoFe moment measured with a SQUID magnetometer at 20 K, where the moment values are scaled for comparison with the P_C curves.

CoFe/MgO injector was used to vary the injection current.

Figure 1 shows representative EL polarization measurements at 100 K for the sample before (■) and after annealing at 340 °C (●). In these measurements a 1.8 V bias voltage was applied. The measured current was 0.12 and 0.10 mA before and after the anneal, respectively. The inset in Fig. 1(a) shows typical EL spectra in perpendicular magnetic fields of −5, 0, and 5 T. The heavy-hole emission at longer wavelengths is well separated from the light-hole emission that appears at shorter wavelengths. Since the electron heavy-hole EL polarization is equal to the spin polarization of the recombining electrons, only the heavy-hole EL polarization, denoted as P_{EL}, will be considered here. The dominance of the left (σ^+) circular component at positive field and the right (σ^-) circular component at negative field indicates majority spin carrier injection, and as expected, the two components are identical in the absence of a magnetic field. The relative intensities of the two circular components determine P_{EL}: $P_{EL} = (I^+ - I^-)/(I^+ + I^-)$ where $I^+(I^-)$ is the intensity of the $\sigma^+(\sigma^-)$ component. As the magnetic field is increased from zero, P_{EL} increases quickly as the CoFe moment is rotated out of plane. After the moment saturates at ∼2 T, P_{EL} continues to increase, but slowly, with field. This slight increase of polarization at high field may be due to field-dependent spin relaxation or electron-hole recombination inside the quantum well. Although the higher polarization at higher fields may more truly reflect the polarization of the injected electrons, the increase in polarization at higher fields is treated here as a linear background contribution and is subtracted from the P_{EL} curves shown in Fig. 1(a) to produce the polarization (P_C) curves plotted in Fig. 1(b). At 100 K, P_C reaches a value of 43% before annealing (□), but increases significantly to 55% after annealing at 340 °C (○). A measurement of the CoFe magnetic moment [carried out with a superconducting quantum interference device (SQUID) magnetometer] with field perpendicular to the sample plane is plotted in Fig. 1(b) (solid lines) with the magnitude scaled
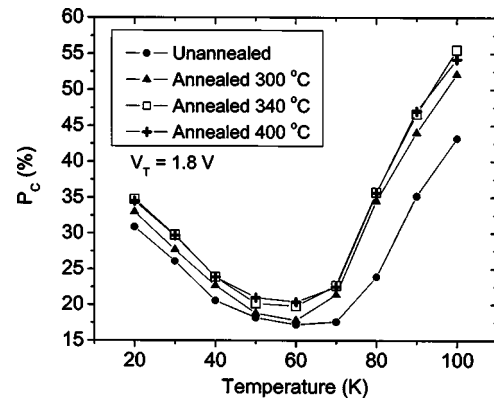

FIG. 2. Measured temperature dependence of P_C at 1.8 V before annealing (●) and after the 300 °C (▲), 340 °C (□), and 400 °C (+) anneals. A significant increase in P_C occurs at temperatures above 70 K after the 300 °C anneal, and subsequent annealing to 340 °C increases P_C slightly at all temperatures. Further annealing up to 400 °C produced only very small additional changes in P_C.

for comparison with the P_C curves. The excellent matching of the SQUID data to the P_C results confirms that the measured polarization derives from the CoFe film layer. To exclude possible artifacts in the experiment, the same measurement was conducted on a control device with a nonmagnetic Pt/MgO injector, which showed only a small $P_{EL}(<1\%)$ that was not field dependent. In addition, photoluminescence experiments indicated that the effects of polarization-dependent absorption and reflection within the CoFe/MgO injector and semiconductor structure are small ($<2\%$).

Figure 2 plots the P_C values for temperatures up to 100 K with $V_T = 1.8$ V before annealing (●) and after the 300 °C (▲), 340 °C (□), and 400 °C(+) anneals. Note that the small confinement potential of the GaAs/Al$_{0.08}$Ga$_{0.92}$As quantum well detector precluded measurements at temperatures greater than ∼100 K. The curves in Fig. 2 closely resemble the temperature dependence of P_C reported in similar devices,[14] which likely derives from changes in both the spin relaxation time and recombination lifetime with temperature within the quantum well.[18,19] Anneals at 180, 220, and 260 °C introduced negligible changes in the EL polarization (not shown). However, annealing at 300 °C produced a pronounced increase in P_C by nearly 10% for temperatures above 70 K, although only a modest improvement in polarization was seen for measurements below 70 K. Further annealing up to 400 °C resulted in marginal additional improvements in P_C at all temperatures (see Fig. 2).

Figure 3 illustrates, more clearly, the temperature-dependent increase in P_C seen after annealing. The change in P_C with temperature is plotted as:

$$\frac{\Delta P_C(T)}{P_C(T)} = \frac{P_C'(T) - P_C(T)}{P_C(T)},$$

where P_C' is the polarization after a respective anneal and P_C is the polarization before any anneal treatments. Since P_C exhibits a strong nonmonotonic temperature dependence, this normalization procedure allows changes in P_C at each temperature to be identified more easily. Since the growth temperatures for the semiconductor heterostructure far exceed the anneal temperatures used in these experiments, the spin-relaxation mechanisms in the quantum well should not change much with these anneal treatments. From Fig. 3,
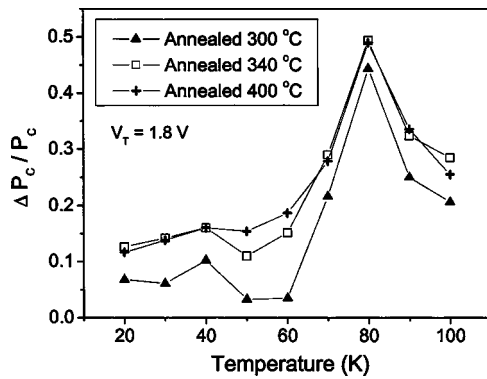
FIG. 3. Temperature dependence of normalized changes in polarization $\Delta P_C(T)/P_C$ between P_C before and after annealing at 300 °C (▲), 340 °C (□), 400 °C (+) for V_T=1.8 V.

$\Delta P_C/P_C$ at temperatures greater than 70 K is noticeable larger than below 70 K, while a spike occurs at 80 K due to a large improvement of P_C. Subsequent anneal treatments at higher temperatures show similar $\Delta P_C/P_C$ behaviors.

The annealing effects on EL polarization, seen in Figs. 2 and 3, merit further discussion. Thermal annealing likely improves the MgO interfaces as well as the quality of the CoFe/MgO(100) tunnel barrier. Changes in the tunnel injector on annealing resulted in successive decreases in tunneling current, at 1.8 V, from 0.12 mA before any anneal treatments to 0.093 mA after the final 400 °C anneal. Improvements in the tunnel spin injector structure with anneal treatments have been found to lead to a more highly spin-polarized current[2] which should thereby lead to increased P_C. However, P_C does not increase systematically at each temperature, but rather there appears to be an unusual temperature dependence to $\Delta P_C(T)/P_C$, as shown in Fig. 3.

One possible explanation for the temperature dependence of the polarization improvement shown in Figs. 2 and 3 is a contribution from a low Curie temperature component to the magnetization of the device. It has been postulated that such a contribution may account for discontinuous increases of TMR with decreasing temperature below ~70 K, sometimes observed in magnetic tunnel junctions (with Al_2O_3 tunnel barriers).[20] Annealing could raise the Curie temperature of this component and thus extend its magnetization contribution to higher temperatures. However, the increase of ΔP_C with temperature seen between 70–80 K is too abrupt to model as such a Curie temperature effect and, moreover, the source of such an effect is unclear.

Another possible explanation for the experimental results are possible variations in electron spin relaxation arising indirectly from thermal annealing. While the semiconductor heterostructure is unlikely changed by the comparatively low-temperature anneal treatments used here, changes in the tunnel barrier could affect the trajectories of the electrons injected across the tunneling barrier. Since the tunneling probability depends exponentially on the tunnel barrier thickness, it is possible that changes in the tunnel barrier structure on annealing alter the angular spread of the cone of injected electrons. Since the relaxation of the electron's spin is strongly dependent on its momentum perpendicular and parallel to the plane of the quantum well structure, changes in the cone angle may well result in changes in

spin relaxation in the semiconductor heterostructure. Since P_C shows a nonmonotonic temperature dependence, changes in spin relaxation could account for the observed changes in P_C with anneal treatments. Indeed, the large spike at 80 K seen in Fig. 3 arises because the increase in P_C with temperature observed at temperatures above ~80 K in the as-deposited sample begins at a lower temperature of ~70 K after the anneal at 340 °C. Similarly, the minimum in $P_C(T)$ shown in Fig. 2 is moved to a lower temperature after annealing. These observations suggest the possible decrease of a temperature at which a specific spin-relaxation mechanism is suppressed by thermal annealing effects.

In conclusion, a tunnel spin injector formed from sputter-deposited CoFe/MgO(100) at room temperature not only exhibits high spin injection efficiency into GaAs at temperatures up to ~100 K (where the measurement temperature is limited by the properties of the quantum well optical detector), but the spin injection efficiency increases when the device is thermally annealed. Heavy-hole electroluminescence polarization values as high as 55% are observed at 100 K after anneal treatments up to 400 °C. Their efficient spin injection and robust thermal stability make CoFe/MgO tunnel spin injectors attractive candidates for spin injection and detection in semiconductor spintronic devices.

[1]D. D. Awschalom, D. Loss, and N. Samarth, in *NanoScience and Technology*, edited by P. Avouris, K. von Klitzing, H. Sakaki, and R. Wiesendanger (Springer, Berlin, 2002).

[2]S. S. P. Parkin, C. Kaiser, A. Panchula, P. Rice, M. Samant, and S.-H. Yang, Nat. Mater. **3**, 862 (2004).

[3]I. Zutic, J. Fabian, and S. Das Sarma, Rev. Mod. Phys. **76**, 323 (2004).

[4]R. Fiederling, M. Kleim, G. Reuscher, W. Ossau, G. Schmidt, A. Wang, and L. W. Molenkamp, Nature (London) **402**, 787 (1999).

[5]B. T. Jonker, Y. D. Park, B. R. Bennett, H. D. Cheong, G. Kioseoglou, and A. Petrou, Phys. Rev. B **62**, 8180 (2000).

[6]Y. Ohno, D. K. Young, B. Beschoten, F. Matsukura, H. Ohno, and D. D. Awschalom, Nature (London) **402**, 790 (1999).

[7]G. Schmidt, D. Ferrand, L. W. Molenkamp, A. T. Filip, and B. J. v. Wees, Phys. Rev. B **62**, R4790 (2000).

[8]E. I. Rashba, Phys. Rev. B **62**, R16267 (2000).

[9]H. J. Zhu, M. Ramsteiner, H. Kostial, M. Wassermeier, H.-P. Schönherr, and K. H. Ploog, Phys. Rev. Lett. **87**, 016601 (2001).

[10]A. T. Hanbicki, O. M. J. van 't Erve, R. Magno, G. Kioseoglou, C. H. Li, B. T. Jonker, G. Itskos, R. Mallory, M. Yasar, and A. Petrou, Appl. Phys. Lett. **82**, 4092 (2003).

[11]T. Manago and H. Akinaga, Appl. Phys. Lett. **81**, 694 (2002).

[12]V. F. Motsnyi, P. V. Dorpe, W. V. Roy, E. Goovaerts, V. I. Safarov, G. Borghs, and J. D. Boeck, Phys. Rev. B **68**, 245319 (2003).

[13]X. Jiang, R. Wang, S. van Dijken, R. Shelby, R. Macfarlane, G. S. Solomon, J. Harris, and S. S. P. Parkin, Phys. Rev. Lett. **90**, 256603 (2003).

[14]X. Jiang, R. M. Shelby, R. Wang, R. M. Macfarlane, S. R. Bank, J. S. Harris, and S. S. P. Parkin (to be published).

[15]W. H. Butler, X.-G. Zhang, T. C. Schulthess, and J. M. MacLaren, Phys. Rev. B **63**, 054416 (2001).

[16]J. Mathon and A. Umerski, Phys. Rev. B **63**, 220403 (2001).

[17]F. Meier and B. P. Zakharchenya, *Optical Orientation* (North-Holland, Amsterdam, 1984).

[18]M. Gurioli, A. Vinattieri, M. Colocci, C. Deparis, J. Massies, G. Neu, A. Bosacchi, and S. Franchi, Phys. Rev. B **44**, 3115 (1991).

[19]V. I. Puller, L. G. Mourokh, N. J. M. Horing, and A. Y. Smirnov, Phys. Rev. B **67**, 155309 (2003).

[20]A. F. Panchula, Ph.D. thesis, *Magnetotransport in Magnetic Nanostructures* (Stanford University, Stanford, CA, 2003).